**Tectonic evolution of syn- to late-orogenic sedimentary-volcanic basins in the central Norwegian Caledonides**

Ella W. Stokke*[1,2], Deta Gasser[3,1], Bjørgunn H. Dalslåen[4] & Tor Grenne[1]

[1]Geological Survey of Norway, P.O. Box, 6315 Torgarden, 7491 Trondheim, Norway

[2]Centre for Earth Evolution and Dynamics (CEED), University of Oslo, PO Box 1028, Blindern 0315 Oslo, Norway

[3]Institute for Natural Sciences, Western Norway University of Applied Sciences, P.O. Box 7030, 5020 Bergen, Norway

[4]Department of Geosciences, University of Oslo, P.O. Box 1047 Blindern, 0316 Oslo, Norway

*Correspondence (e.w.stokke@geo.uio.no)

Abbreviated title: Tectonic evolution of Dugurdsknappen

**Abstract:** We present new structural, geochemical, and U-Pb zircon data from syn- to late-orogenic sedimentary-volcanic basins in the southwestern part of the Trondheim Nappe Complex (TNC), central Norwegian Caledonides. In this area, a succession of E-MORB type metabasalt, jasper, ribbon chert with associated sandstone and conglomerate, and green siltstone is interpreted to represent volcanism and sedimentation in a hitherto little known spreading-dominated tectonic environment. This environment is different from the supra-subduction zone ophiolite setting dominating the Iapetus rock record elsewhere in the Scandinavian Caledonides. This volcanic and sedimentary succession was overturned and isoclinally folded in a pre-427 Ma orogenic phase. Post-427 Ma cross-bedded sandstones were deposited on the eroded surface of the previously deformed rocks, representing a rare example of a late Silurian or younger sedimentary basin within the Scandinavian Caledonides. The cross-bedded sandstones are intercalated and/or overlain by post-427 Ma intermediate volcanic/subvolcanic rocks of calc-alkaline composition, representing a hitherto unknown volcanic phase within the TNC and elsewhere within the Scandinavian Caledonides. Their particular geochemical signature could be the result of late-stage subduction zone volcanism just prior to the onset of continent-continent collision between Baltica and Laurentia, or much younger post-collisional extensional melting with inherited subduction signatures.

**Supplementary material:** Description of analytical methods and table with geochronological data from LA-ICP-MS analysis of zircons are available at xx.

In his seminal paper on the Caledonian rock record, Wilson (1966) proposed the existence of a Palaeozoic "proto-Atlantic" ocean, which further led him to propose the famous Wilson cycle, describing the cyclic opening and closure of oceanic basins due to plate tectonic movements. Wilson's proto-Atlantic ocean was later termed Iapetus (Harland & Gayer 1972). This ocean opened due to the break-up of Rodinia in the Late Neoproterozoic, and closed during the convergence and final collision of Baltica, Laurentia, and Avalonia from the Late Cambrian to the Devonian, leading to the formation of the Caledonian orogen (e.g. Gee *et al.* 2008; Corfu *et al*. 2014). Based on detailed palaeontological, stratigraphic, geochemical, geochronological, and paleomagnetic data from Iapetus remnants preserved within the Caledonian orogen, a continuously better understanding of the opening and closure history of this important ancient oceanic basin has evolved (e.g. Neuman 1984; Dunning & Pedersen 1988; Torsvik & Trench 1991; Pedersen *et al.* 1992; Harper *et al.* 1996; Mac Niocaill *et al.* 1997; Domeier 2016).

One particular area where large remnants of the Iapetus basin are preserved and important aspects of its evolution have been resolved, is within the Trondheim Nappe Complex (TNC) of the central Norwegian Caledonides (Fig. 1). Within the Løkken-Vassfjellet-Bymarka area in the western part of this nappe complex (Fig. 2), ophiolitic fragments (here referred to as the LVB ophiolites), were deformed and obducted onto an unknown landmass during an early Ordovician tectonic event (the "Trondheim disturbance", e.g. Holtedahl 1920; Vogt 1945), representing an important orogenic phase prior to the final Caledonian (Scandian) continent-continent collision (Roberts 2003). Unconformably overlying the deformed LVB ophiolites, the sedimentary and volcanic rocks of the Lower and Upper Hovin and Horg Groups were used to derive a model for subsequent volcanic arc development and basin infill, possibly stretching into the Middle Silurian (e.g. Bruton & Bockelie 1980; Grenne & Roberts 1998; Gasser *et al*. 2016).

Despite its central position within the Scandinavian Caledonides and its importance for reconstructing the closure history of the Iapetus Ocean, several aspects of the tectonic evolution of the western TNC are far from resolved. These are in particular: (1) Are all major metabasaltic units of the area correlatable ophiolite fragments that represent one phase of oceanic crust production? And (2) are all sedimentary successions exposed within this area coeval deposits and part of the same Hovin-Horg basin system? Answering these questions is mainly hampered by the limited geographical extent of detailed geological investigations in the western TNC, which so far has been concentrated mainly in the northwestern parts between Løkken, Støren, and Trondheim (Fig. 2a).

The large area to the southwest, from Ilfjellet to Hjerkinn (Fig. 2a), has so far received very little attention and the age and tectonic setting of the metabasaltic and metasedimentary rocks in this area are unknown. Nevertheless, on published large-scale maps, these metabasaltic rocks have been correlated with the LVB ophiolites, and the metasedimentary rocks with the Hovin and Horg Groups (Fig. 2a; Wolff 1976; Nilsen & Wolff 1989). Rohr-Torp (1972) also suggested that the entire metabasaltic-metavolcanic sequence in this area lies in an overturned position (Fig. 2b). The aim of this contribution is to provide detailed field observations, and geochemical and geochronological data from a key area covering both the metabasaltic and sedimentary units within this southwestern part of the TNC: the Dugurdsknappen area (Fig. 2a). Our results have implications for previous correlations and point to a more complex evolution of Iapetus closure in the western TNC than previously envisaged.

## Geological setting

The Trondheim Nappe Complex (Figs. 1, 2a) is preserved within a large-scale NNE-SSW trending structural depression in central Norway and consists of various volcanic and sedimentary units arranged in subparallel belts (Fig. 2a; Roberts & Wolff 1981; Gee *et al.* 1985; Grenne *et al.* 1999). The central belt consists of the sediment-dominated, highly deformed and relatively high-grade Gula Complex (Fig. 2a). To the west and east there are less deformed and generally lower grade volcanic and sedimentary belts commonly referred to as the Støren and Meråker Nappes, respectively (Fig. 2a; Gee *et al.* 1985).

The western belt, which is relevant for this contribution, has traditionally been divided in two lithologically contrasting parts (Fig. 2a): (1) Metabasaltic sequences (including the LVB ophiolites) collectively assigned to the so-called Støren Group (e.g. Wolff 1979; Gee *et al.* 1985), in the following referred to as the Støren Group *sensu lato* (*s.l.*), and (2) an overlying sediment-dominated succession subdivided into the Hovin and Horg Groups (e.g. Vogt 1945; Wolff 1979). The LVB ophiolites, constituting the northwestern parts of the Støren Group *s.l.* (Fig. 2a), include gabbros, sheeted dykes and pillow lavas (Grenne *et al.* 1980, Heim *et al.* 1987; Grenne 1989) dated at 487-479 Ma (Roberts *et al*. 2002; Slagstad *et al*. 2013). Based primarily on volcanic geochemistry, these ophiolites are thought to represent fragments of a marginal basin in a supra-subduction zone setting (Grenne 1989; Grenne *et al.* 1999; Slagstad

2003). By contrast, recent work by Grenne & Gasser (2017) shows that the southeastern belt of metabasalts and thin intercalated metasediments running from Ilfjellet through the town of Støren and northwards to Mostamarka (Fig. 2a), referred to in this paper as the Støren Group *sensu stricto* (*s.s.*), is lithologically and geochemically different from the LVB ophiolites, and hence may represent a separate tectonic setting. How this Støren Group *ss* relates to the metabasalts and metasedimentary rocks south of Ilfjellet, is unknown at present.

The thick succession of conglomerates, sandstones, shales, limestones, and intercalated volcanic rocks assigned to the Hovin and Horg Groups (Fig. 2a) lies unconformably above the metabasaltic and partly ophiolitic sequences, separated by an assumed orogenic event originally referred to by Vogt (1945) as the "Trondheim Disturbance". Various stratigraphic schemes (e.g., Chaloupsky 1970; Oftedahl 1980; Oftedahl & Prestvik 1985; Walsh 1986, Gasser *et al.* 2016) have been proposed since Vogt's (1945) original subdivision of this 'post-Støren' sedimentary and volcanic succession. In the lower parts, emplacement of felsic and intermediate rocks at about 468-467 Ma indicate volcanic arc development subsequent to accretion of the LVB ophiolites (Grenne & Roberts 1998; Roberts *et al.* 2002; Slagstad *et al.* 2013). Middle Ordovician (*c.* 463-467 Ma) fossils in the Hølonda limestone show Laurentian affinities (Neumann & Bruton 1989; Harper *et al.* 1996) and are coeval with the extrusion of intermediate volcanic rocks (Bruton & Bockelie 1980) with a subduction-related, shoshonitic affinity (Grenne & Roberts 1998). Upper Ordovician (Late Caradoc to Early Ashgill) fossils (Neumann *et al.* 1997) are found in a part of the sequence that also contains extensive rhyolites (Roberts *et al.* 1984), and recent studies of detrital zircon in sandstones and conglomerates indicate that the stratigraphy extends well into the Silurian (<430 Ma; Gasser *et al*. 2016).

A 1:250.000 scale map of the presently studied area (Nilsen & Wolff 1989) shows a succession of 'green banded tuffite and green phyllite' intercalated with metabasaltic volcanic rocks, interpreted as a correlative of the Støren Group *s.l.* to the north, as well as a metasedimentary succession of 'green greywacke and shale' that has been loosely correlated with the Hovin groups (Fig. 2a; Nilsen & Wolff 1989). Rohr-Torp (1972) interpreted a conglomerate between the metavolcanic and the metasedimentary succession as representing an erosional contact, and, based on limited way-up observations he considered the entire succession to be inverted and folded into upright folds (Fig. 2b).

## Geology of the Dugurdsknappen area

Our recent mapping shows two major units within the Dugurdsknappen area, separated by a major unconformity: (1) strongly deformed metabasalts, cherts, and siliciclastic rocks, overlain by (2) less deformed siliciclastic and intermediate volcanic and or subvolcanic rocks (in the following referred to as just intermediate volcanic rocks; Fig. 3).

### *Lithologies below the unconformity*

The metabasaltic rocks below the unconformity are dominated by pillow lavas (Figs. 3, 4a) and massive flows, as well as small pockets of gabbro and zones of mafic lavas with a bleached and altered appearance (Fig. 3). Most pillow structures are strongly deformed; however, local well preserved pillows indicate way up towards a succession of ribbon chert and siltstone (Fig. 3). There are also accumulations of volcaniclastic deposits composed of basaltic material, particularly towards the chert. Between metabasalts and ribbon chert, local accumulations of jasper (Figs. 3a) are interpreted to mark the stratigraphic top of basaltic lava flows. The overlying succession of ribbon chert (Fig. 4b) has intercalated beds of immature sandstone and light-coloured polymictic conglomerate (Fig. 4c). Stratigraphically upwards, the ribbon chert grades into silty chert and further up into green siltstone (Fig. 3), indicating a gradually decreasing chert production.

### *Lithologies above the unconformity*

A green cross-bedded sandstone, typically medium- to coarse-grained and poorly sorted, is exposed directly above the unconformity (Fig. 3a). Near its base, it contains abundant, scattered, up to 10 cm large rounded clasts of felsic plutonic rocks and quartzite. Locally, there are also denser-packed conglomeratic layers containing angular chert clasts (Figs. 3, 4d). Further up from the unconformity, the sandstone shows well-preserved cross-bedding and occurrences of trough cross-bedding (Figs. 3, 4e). Intermediate volcanic rocks appear as sheets in the sandstones above the unconformity and as dykes cutting the underlying sequence (Figs. 3, 4f). These massive, light greenish igneous rocks have a porphyritic texture with large biotite phenocrysts in a fine-grained, light matrix (Fig. 4g).

### *Deformation and metamorphism*

Below the unconformity, the map pattern defines a large-scale, upright, isoclinal fold structure (Fig. 3a, b). Measurements of bedding planes, observed mostly in ribbon chert and siliciclastic rocks, scatter along a great circle indicating that the fold axis of this large-scale fold plunges S-SE (Fig. 5a). Measurements of outcrop-scale fold axes below the unconformity scatter considerably and plunge moderately SE to SW (Fig. 5b). Observations within the ribbon chert (Fig. 4h) show that tight to isoclinal folds with axes plunging to the S-SE are refolded by folds with axes plunging to the SW, indicating that the outcrop-scale folds belong to two distinct fold phases; S-SE trending F2 folds and SW trending F3 folds (Fig. 3a). All units below the unconformity show a prominent, moderately SE-dipping spaced to penetrative foliation, which is axial planar to the SW-trending F3 folds (Fig. 5c) and cuts obliquely through the large-scale isoclinal fold structure (Fig. 3a). No evidence of an older foliation related to the SE-plunging F2 folds has been observed.

The general map pattern shows that the base of the cross-bedded sandstone cuts obliquely through the isoclinally folded succession below, demonstrating that the boundary represents a major unconformity (Fig. 3). However, the unconformity and the units above are folded and foliated as well: bedding planes above the unconformity scatter along a great circle indicating a large-scale fold axis plunging moderately S-SW (Fig. 5d), consistent with measured axes of outcrop-scale folds (Fig. 5e), and in accordance with the F3 fold phase. The outcrop-scale folds are mainly open to close, with SE-dipping axial planes and a dominant NW vergence (Figs. 4i, 5f). Both the sandstone and the volcanic rocks show a spaced to penetrative foliation dipping SE, axial planar to the SW-trending F3 folds (Fig. 5f). The intensity of folding and foliation increases towards and southwards along the unconformity, resulting in subvertical bedding and foliation orientations on both sides, making it locally difficult to identify the unconformable relationship (Fig. 3c).

The similarity in orientation of SW-plunging, NW-verging F3 folds with associated axial planar foliation both below and above the unconformity indicates that this folding phase post-dates the formation of the unconformity. The spaced to penetrative foliation is associated with greenschist facies metamorphism, indicated by chlorite/epidote and biotite/sericite mineral growth along foliation planes in metabasalts and siliciclastic rocks, masking any potential pre-existing metamorphic break across the unconformity.

**Geochemistry of igneous rocks**

Whole-rock major and trace element geochemistry of igneous rocks was obtained from both sides of the unconformity. The samples include seven metabasaltic, one gabbroic, and one intermediate dyke from below the unconformity, and four intermediate volcanic rocks from above the unconformity, all analysed by XRF and laser ablation ICP-MS (Table 1; Fig. 3a); see Supplementary material for detailed analytical techniques. All metabasaltic and gabbroic samples from below the unconformity have typical basaltic major element compositions, with $SiO_2$ values ranging from 47.6-50.4 wt% (Table 1) and <53% when recalculated on a volatile-free basis (Fig. 6). The intermediate volcanic rocks from above the unconformity and the intermediate dyke from below the unconformity have $SiO_2$ values ranging from 52.5 to 58 wt% (Table 1) and plot as andesitic rocks on a volatile-free basis (~57-61% $SiO_2$; Fig. 6).

Trace element concentrations from all the igneous samples are shown in MORB (Mid Ocean Ridge Basalt)-normalized multi-element plots (Fig. 7a) including only high field strength elements (HFSE), which are considered stable during greenschist facies metamorphism (Pearce 1982). The analysed samples fall into two categories: (1) Metabasalts and gabbro below the unconformity show a negative slope from Th (most incompatible HFSE) to Hf, followed by a continued negative gentle slope from Sm to Yb (Fig. 7a), a pattern typical of oceanic rift related rocks (e.g. Pearce 1982). (2) The intermediate volcanic rocks above the unconformity and the dyke from below show strong enrichment of Th and a characteristic negative Ta and Nb anomaly (Fig. 7a), a pattern that is comparable to those of typical calc-alkaline, volcanic arc rocks (Pearce 1982; Fig. 7a).

Chondrite-normalized rare earth element (REE) patterns (Fig. 7b) again show two distinct trends. (1) The metabasalts and gabbro below the unconformity show moderate enrichment of the light REE (LREE) with a fairly even and gentle negative slope towards the heavy REE (HREE), typical for enriched MORB (E-MORB) basalts (Fig. 7b; Winter 2010). Such REE patterns exist in basalts of different tectonic settings, but are particularly common in marginal basin basalts (Wilson 1989, p. 236). (2) The intermediate volcanic rocks above the unconformity and the related dyke show a stronger LREE enrichment and a steeper negative slope from La to Gd (Fig. 7b).

A Ti-Zr-Y ternary plot (Fig. 8a) discriminates particularly well between within-plate basalts on the one hand and arc tholeiites, ocean floor tholeiites, and calc-alkaline arc basalts on the other hand; the latter three types being partly overlapping and less distinctive (Pearce and Cann 1973). All metabasalts and gabbro samples from below the unconformity plot in the field of ocean-floor basalts, while the intermediate volcanic rocks above the unconformity and the intermediate dyke plot in the calc-alkali basalt field. A Zr vs-Ti plot (Fig. 8b, Pearce and Cann 1973) is consistent with the above, showing that the metabasalts and gabbro all plot within the MORB field, while the intermediate volcanic rocks and the dyke plot in the calc-alkali field (Fig. 8b). The ternary Th-Ta-Hf discrimination diagram of Wood (1980), which discriminates particularly well between arc-related and different types of rift-related volcanic rocks even for intermediate to felsic compositions, shows that the metabasalts and the gabbro have E-MORB basaltic compositions typical of oceanic rift settings. In marked contrast, the intermediate volcanic rocks and the dyke have a clear volcanic arc affinity (Fig. 8c) consistent with the calc-alkaline compositions noted above.

## Geochronology

Two samples were collected for zircon geochronology in order to constrain the depositional age of the rocks above the unconformity. The zircons were separated using conventional magnetic and heavy liquid techniques, and analysed for U-Pb concentrations using laser ablation ICP-MS; see Supplementary material for detailed analytical techniques.

The first sample, EST_12, is a light coloured coarse-grained tonalitic clast, rounded and about 10 cm in diameter, taken from the lower conglomeratic part of the cross-bedded sandstone (Fig. 3). A total of 136 zircons were found, comprising relatively large (up to about 150 µm) grains of clear to light yellow colour with abundant fractures and inclusions. Cathodoluminescence (CL) images reveal that most of the zircons have a very dark core surrounded by a relatively broad and light coloured rim with varied zoning (Fig. 9a). For this sample a total of 25 analyses were done on 23 grains; 15 analyses on the cores and 10 on the rims. Of the 25 analyses, 11 core analyses had very high uranium content, causing the detector of the ELEMENT 2/XR-instrument to switch from a counting mode to an analogue mode, resulting in poor linearity between low- and very high count-rates, and overestimation of the U/Pb age. The analyses derived in analogue mode were therefore omitted, together with two analyses that were >10% discordant. The remaining analyses include four from the cores and eight from the rims (Fig. 9b). All these data overlap and give a concordia age of 485 ± 4 Ma, which we interpret as the crystallisation age of the tonalitic clast and hence a maximum age for the deposition of the sandstone.

The second sample, EST_112, is from the cross-bedded sandstone (Fig. 3). A total of 146 zircons were picked; generally clear and well preserved, and up to 200 µm long with mainly euhedral shape and slightly rounded edges. The CL images revealed a large variety of zoned grains, in addition to a few with unzoned, patchy, or a core-rim structure (Fig. 10a). Of the 100 analyses performed on 100 grains, 10 show >10% discordance and were discarded, while the remaining 90 analyses are <10% discordant. There are three main age groups, with hiatuses in between (Fig. 10b). The smallest and oldest group consists of three Palaeoproterozoic and two

Archean grains. The largest group includes ages of ~900-2000 Ma, with a big peak at 1100 Ma and smaller ones at ~900 and 1740 Ma, and a hiatus at ~1260-1300 Ma. The youngest group is ~420-500 Ma, with smaller peaks (minimum 3 grains) at around 430, 460 and 490 Ma, and hiatuses at ~430-440 and 465-470 Ma (Fig. 10c). The youngest population is estimated from the youngest significant peak comprising five overlapping concordant grains, according to recommendations of Dickinson & Gehrels (2009). This group has a concordia age of 427 ± 3 Ma (Fig. 10d), which represents a conservative estimate for the maximum depositional age of the sandstone (Dickinson & Gehrels 2009).

## Tectonic evolution of the Dugurdsknappen area

### *1. Basaltic volcanism with subsequent chert and siltstone sedimentation*

The geochemistry of metabasalts and gabbro below the unconformity points to E-MORB compositions, with no island arc or subduction zone signatures (Figs. 7, 8). This suggests that these rocks formed along a spreading ridge, in either a major ocean or a marginal basin. White ribbon cherts are found as thin layers and pockets within the metabasaltic unit and as a thick package above. Their presence both between and above the metabasalts indicates that chert sedimentation occurred both during quiet intervals between volcanic events and after volcanism had ceased. Chert sedimentation indicates little detrital input to the basin at the time, as chert is composed of silica most commonly originating from biogenic sources like radiolarians and sponge spicules (Jones & Murchey 1986; Pufahl 2010). It has been suggested that Ordovician to lower Cretaceous radiolarian cherts typically formed in response to upwelling of nutrient-rich waters, conditions which can be caused by specific tectonic environments, such as the local upwelling seen in marginal basins in modern oceans (Jones & Murchay 1986). A marginal basin setting for the ribbon chert is supported by the abundant intercalated beds of coarse terrigenous sandstone and mass flow type conglomerates, which suggest proximity to a terrigenous source. The upwards transition into the thick succession of green siltstone suggests a gradual decrease of both radiolarian chert production and coarse terrigenous input, possibly due to a change in basin geometry and/or changes in the hinterland.

### *2. Overturning (D1) and major folding (D2)*

The metabasalts – ribbon chert – green siltstone succession is folded into a tight to isoclinal, upright fold with a S-SE-plunging fold axis, resulting in a map pattern with older metabasalts surrounding the younger lithologies in the south (Fig. 3a). The younging direction towards the central siltstone together with the south-plunging fold axis, indicate that this fold structure cannot represent a simple syncline, but rather a moderately south-plunging antiformal syncline (Fig. 3b). This implies an overturning (D1) of the stratigraphic sequence below the unconformity, possibly as part of a large-scale recumbent fold nappe, prior to tight, upright S-SE plunging F2 folding (D2). Importantly, both the D1 overturning and the D2 upright folding must have taken place before erosion and deposition of the cross-bedded sandstone above the unconformity. This differs from the interpretation of Rohr-Torp (1972), who interpreted the cross-bedded sandstone to be part of the overturned sequence (Fig. 2b).

*3. Shallow-water sandstone deposition*

The immature and poorly sorted nature of the green, cross-bedded sandstone above the unconformity, including abundant larger clasts, indicates a relatively proximal, shallow-water deposition. Sedimentary structures such as laterally extensive parallel bedding, lamination, abundant cross-bedding, and occasional trough cross-bedding also suggest a marine shelf setting above wave base, possibly upper shoreface (Tucker 2001; Boggs 2011). The unit has previously been classified as a greywacke (Rohr-Torp 1972; 1974), a rock type commonly related to arc basins, including piggy-back basins and similar settings (Tucker 2001). The detrital zircon spectrum of the sandstone indicates deposition of this sandstone after *c.* 427 Ma (Fig. 10d), post-dating mid Silurian times.

*4. Late intermediate volcanism*

The younger volcanic rocks at Dugurdsknappen show a geochemical signature clearly different from the older metabasalts, indicating a change in tectonic environment across the unconformity. Since the intermediate volcanic rocks are coeval or younger than the cross-bedded sandstone, they also must have formed after *c.* 427 Ma. These volcanic rocks have an intermediate composition with trace element compositions similar to calc-alkaline magmas (Figs. 7, 8). A calc-alkaline affinity is supported by the presence of biotite phenocrysts, typical of more evolved silicic rocks such as basaltic andesites, andesites, dacites, and rhyolites, particularly those of the medium to high K-series (Winter 2010; Nesse 2013). The calc-alkaline series is typical of supra-subduction zone settings at destructive plate boundaries (Winter 2010). The negative Ta-Nb anomaly seen in the trace element patterns (Fig. 7a) is also typical of subduction-related rocks (Wilson 1989, p. 179; Winter 2010); however, geochemically comparable magmas may also form in collisional orogenic belts (Harris *et al.* 1986). Such late- to post-collisional calc-alkaline magmas have been linked to transtensional and transpressional tectonism during the phase of extensional collapse at the end of an orogenic cycle, leading to upwelling and partial melting of previously contaminated mantle (Harris *et al.* 1986; Song *et al.* 2015). Contamination is typically due to previous subduction zone activity, which leads to the apparent subduction-zone signature (Harris *et al.* 1986; Miles *et al.* 2016).

*5. Renewed folding and development of the regional foliation (D3)*

Both the units below and above the unconformity were affected by a deformation phase characterised by SW-trending NW-vergent F3 folding (D3; Fig. 4i, 5d, e). This third deformation event is most pronounced along the unconformity and in the lower part of the cross-bedded sandstone, but it is also seen overprinting previous F2 folding within the ribbon chert (Fig. 5b). The regional foliation, which can be observed both above and below the unconformity, is parallel to the axial plane of F3 folds and cuts across the hinge and flanks of the large-scale D2 fold below the unconformity (Figs. 3a, 5c, f). We therefore interpret the regional foliation to have formed during the D3 event. Interestingly, the orientation and vergence of D3 structures does not fit with the general SE-directed nappe translation and deformation during the main collisional stage of the Scandinavian Caledonides, so they either represent structures developed during back-thrusting, or during late and post-Caledonian top-to-the-west extensional tectonics (e.g. Fossen 1992).

## Consequences for along-strike correlations within the TNC and regional-scale significance for the evolution of the Caledonian orogen

The Dugurdsknappen area represents only a small part of the southwestern volcanic and sedimentary belt of the TNC; nevertheless, its tectonic evolution as documented in this study has consequences for along-strike correlations with the better-known northwestern areas, and reveals some important new data relevant for the closure history of the Iapetus and the evolution of the Scandinavian Caledonides in general.

*Late Cambrian to Ordovician basaltic volcanism in the western TNC – two different phases and/or tectonic environments?*

Gasser & Grenne (2017) proposed that the thick metabasaltic sequences in the 'classical' Støren-Hølonda region of the TNC, traditionally collectively assigned to the Støren Group (*s.l.*) of assumed latest Cambrian – earliest Ordovician age (e.g. Wolff 1979; Gee *et al.* 1985; Roberts *et al.* 2002; Slagstad *et al.* 2013), can be divided into two lithologically and geochemically different units; a southeastern Støren Group *s.s.* and a northwestern group comprising the LVB ophiolites. The LVB ophiolites show a clear subduction signature (such as elevated Th/Ta ratios, Slagstad *et al.* 2013), a signature which is absent in the data from the Dugurdsknappen and Støren Group *s.s.* metabasalts. Moreover, the Dugurdsknappen and Støren Group *s.s.* metabasalts share an enrichment in LREE and the most incompatible HFSE, a signature that is apparently absent in the LVB ophiolites (Slagstad *et al.* 2013, Grenne & Gasser 2017). We therefore suggest that the Dugurdsknappen and Støren Group *s.s.* metabasalts originate from the same volcanic environment, different from the environment in which the LVB ophiolites were produced.

The LVB ophiolites formed at *c*. 487–479 Ma in the latest Cambrian to early Ordovician period, most probably in a back-arc extensional basin in a suprasubduction zone setting (Slagstad *et al.* 2013), thus representing suprasubduction-zone (SSZ) ophiolites in the classification of Dilek & Furnes (2011). They belong to an extensive belt of SSZ ophiolites preserved within the Scandinavian Caledonides from Lyngen in the north to Karmøy in the south (Fig. 1; Dunning & Pedersen 1988; Grenne *et al.* 1999; Dilek & Furnes 2011). The Dugurdsknappen and Støren Group *s.s.* metabasaltic belts, by contrast, lack a traditional ophiolite stratigraphy, and a full evaluation of their petrogenesis and tectonic setting is therefore difficult. Nevertheless, their geochemical signature points to a subduction-unrelated environment, suggesting the following possible settings according to the scheme of Dilek & Furnes (2011): Disrupted remnants of Mid-ocean ridge (MOR) type ophiolites formed at plume-proximal or plume-distal mid-ocean ridges, trench-proximal mid-ocean ridges, or trench-distal back-arc spreading ridges. Due to the lack of age control on the Dugurdsknappen and Støren Group *s.s.* metabasalts so far, the paleogeographic significance of this finding is highly speculative, with three main potential models: (1) If they are older than the SSZ ophiolites, they may represent fragments of true Cambrian Iapetus MORB, (2) if they are broadly coeval with the SSZ ophiolites, they may represent a more arc-distal part of the same back-arc basin or a trench-proximal mid-ocean ridge on the down-going plate, or (3) if they are younger than the SSZ ophiolites, they may represent a true extensional interim rifting phase after the first late Cambrian – early Ordovician subduction phase producing the SSZ ophiolites. In any case, they represent a separate tectonic environment and/or phase so far not considered in the closure history of the Iapetus ocean as preserved within the Scandinavian Caledonides.

*Post-mid Silurian sedimentation – a missing link to Old Red Sandstone deposition?*

According to the existing 1:250 000 bedrock map, the cross-bedded sandstone above the unconformity at Dugurdsknappen belongs to a larger, *c.* 8 km wide, restricted circular unit mapped as green greywacke and shale (Fig. 2; Nilsen & Wolff 1989). Based on the occurrence of what Rohr-Torp (1972) interpreted as a basal conglomerate, he correlated this sedimentary unit with the Hovin Groups in the northwestern TNC (Fig. 2). The results of our study clearly indicate that such a correlation is wrong. The sedimentary and volcanic rocks of the Hovin Groups above the LVB ophiolites have a complex stratigraphy, including several conglomerate horizons, and they are assumed to span from the Lower to the Upper Ordovician (e.g. Vogt 1945; Chaloupsky 1970; Oftedahl 1980). The cross-bedded sandstones at Dugurdsknappen, however, have a maximum depositional age of 427±3 Ma, indicating deposition no earlier than mid Silurian times. It is therefore evident that this unit was deposited at a much later stage than most of the Ordovician sediments of the northwestern TNC; hence, they cannot be directly correlated. It is noteworthy, though, that a recent study identified <430 Ma rocks in the northwestern TNC as well: The Lyngestein and Sandå units of the Hovin-Horg area have maximum depositional ages of *c.* 430 Ma (Gasser *et al.* 2016), and are possible time equivalents of the Dugurdsknappen sandstone although they are lithologically different.

Silurian sedimentary rocks are known from several tectonostratigraphic levels within the Scandinavian Caledonides (e.g. Bassett 1985), but successions proven to be as young as <430 Ma (mid-Wenlock or younger) are rare. In the parautochthonous Oslo region, the Ordovician – Silurian stratigraphy extends into the late Silurian, with the Ringerike Group representing shallow-marine to fluvial deposits of <430 Ma (Ludlow-Pridoli) age (Fig. 1; Davies *et al.* 2005; 2006). The Ringerike Group has been interpreted to represent a molasse deposit formed in response to the continental collision between Baltica and Laurentia, and marks the transition from the Cambro-Silurian mainly marine platform of Baltica, to the mainly continental Old Red Sandstone deposits of late Silurian to Devonian times (e.g. Basset 1985; Bruton *et al.* 2010). In the parautochthonous to lower allochthonous Jämtland region (Fig. 1), the Ordovician – Silurian stratigraphy extends only into early Wenlock times, when the basin was filled up with terrestrial Old Red Sandstone deposits (Bassett 1985; Gee *et al.* 2014). Also within the allochthonous Iapetus-derived nappes, fossil evidence indicates that most known Ordovician – Silurian successions extend only into the Llandovery or early Wenlock; however, non-fossiliferous clastic successions that overlie Llandovery – Wenlock rocks are known locally (e.g. within the Lower Köli Nappes; Fig. 1), possibly indicating a more wide-spread presence of <430 Ma deposits (Bassett 1985; Roberts & Stephens 2000; Gee *et al.* 2014).

The discovery of <430 Ma sedimentary basins bounded by major unconformities at Dugurdsknappen (this study) and Lyngestein/Sandå (Gasser *et al.* 2016) is interesting for further tectonic reconstructions for two reasons. (1) The stratigraphic record within such basins might cover a time span transitional from the mainly marine Cambro-Silurian sedimentation within Iapetus to the continental Old Red Sandstone facies, and hence represent a missing link within the closure history of the Iapetus. (2) These basins developed during ongoing thrust tectonics and nappe assemblage, and their extent as well as stratigraphic and tectonic relationships to surrounding structures can potentially reveal important clues about tectonic uplift and subsidence during foreland-propagating deformation in a continental collision zone. The extent, stratigraphic record, depositional age, provenance and structural history of such <430 Ma basins therefore deserve much more attention in the future.

*Post-427 Ma intermediate calc-alkaline volcanism – subduction-related or post-collisional?*

The intermediate volcanic rocks emplaced above the unconformity are either coeval with or younger than the cross-bedded sandstone; hence, they also have a maximum age of about 427 ± 3 Ma. Subduction-related intermediate volcanism has been described from several places within the TNC, but all are older magmatic phases (e.g. Grenne *et al.* 1999). The youngest magmatic phase previously documented in the TNC, comprising plutonic rocks of a bimodal mafic/trondhjemitic assemblage (Grenne et al. 1999), occurred at about 435-430 Ma and includes the Innset massif near Dugurdsknappen (Fig. 2a; Dunning & Grenne 2000; Nilsen *et al.* 2007). The post-427 Ma volcanic rocks (this study) thus represent the youngest magmatic rocks discovered within the TNC so far.

The geochronological database covering all published age determinations from the entire Scandinavian Caledonides contains 53 U-Pb zircon ages younger than 427 Ma (http://geo.ngu.no/kart/geokronologi_mobil/). Most of them (34 ages) represent 410-390 Ma granitic pegmatites or leucosomes from within the Precambrian windows, including the Western Gneiss Region (WGR; Fig. 1). These are probably linked to collisional rather than subduction-zone processes, representing partial melting coeval with or subsequent to eclogite facies metamorphism (e.g. Kylander-Clark & Hacker 2014). The remaining 19 ages represent granitic to granodioritic pegmatites and leucosomes from several allochthonous nappes, possibly representing two age groups: (1) 425-418 Ma pegmatites from mainly northern Norway, reflecting partial melting during nappe thrusting (e.g. Corfu *et al.* 2011), and (2) 405-390 Ma pegmatites from nappes overlying the WGR, interpreted to be part of the underlying collisional pegmatite suite from within the WGR (e.g. Gordon *et al.* 2013). None of these dated rocks correspond lithologically or geochemically to the post-427 Ma volcanic rocks discovered at Dugurdsknappen, and this unit therefore seems to represent a hitherto unknown volcanic unit within the Scandinavian Caledonides.

The subduction-related geochemical signature of this post-427 Ma volcanic unit is difficult to interpret without a precise age of emplacement, and we envisage two potential models. (1) The subduction signature could represent a link to an active subduction zone, a model implying that subduction continued until at least after 427 Ma within this part of the Scandinavian Caledonides. It has been suggested that subduction and arc volcanism within the Scandinavian Caledonides ceased after the onset of continent-continent collision (Bingen & Solli 2009); however, the exact timing of this transition is unknown. Magmatic bodies as young as 424 Ma preserved within the mature volcanic arc in the Helgeland Nappe Complex (Fig. 1; Barnes *et al.* 2007), may suggest that arc magmatism was still active. This model is preferable for the Dugurdsknappen volcanic rocks if they were emplaced at *c.* 427 Ma or slightly later. (2) Alternatively, if the age of emplacement is significantly younger, the subduction signature could be inherited from a mantle modified by a previously active subduction zone, in which case magma generation was unrelated to ongoing subduction processes and rather reflects post-collisional (extensional) melting of mantle rocks. Indeed, post-collisional Middle Devonian calc-alkaline magmatism is known from the British Caledonides (Soper & Woodcock 1990; Miles *et al*. 2016; Lancaster *et al.* 2017). This has been attributed to the re-melting of crustally contaminated mantle during Devonian rifting and extensional collapse, rather than subduction zone magmatism, as it post-dates the final closure of the Iapetus Ocean (Miles *et al*. 2016; Lancaster *et al.* 2017). Such late to post-collisional calc-alkaline magmatism has been described from several orogens around the world (Harris *et al.* 1986; Song *et al.* 2015; Miles *et al.* 2016). Until the emplacement age of the post-427 Ma intermediate volcanic rocks is determined precisely, both a late subduction-zone origin and a potentially much younger post-collision extensional origin has to be considered for this hitherto undocumented calc-alkaline volcanic episode within the Scandinavian Caledonides.

## Conclusions

The oldest rocks in the Dugurdsknappen area are tholeiitic, E-MORB type metabasalts. Geochemical signatures suggest that the Dugurdsknappen metabasalts correlate with the Støren Group *s.s.* metabasalts, and that both are different from the better-known supra-subduction zone ophiolite fragments dominating the oceanic crust record elsewhere within the Scandinavian Caledonides. The Dugurdsknappen and Støren Group *s.s.* metabasalts possibly represent fragments of MOR-type ophiolites, indicating the presence of a hitherto unknown tectonic environment and/or phase of oceanic crust production during the closure of Iapetus. The overlying ribbon chert, intercalated with coarse clastic material, indicates arc- and/or continent-proximity during or shortly after the rift-related volcanism. The gradual transition to the overlying siltstone unit suggests an environment with decreasing chert production in favour of siliciclastic silt deposition, possibly due to a change in basin geometry and/or the hinterland.

The Dugurdsknappen metabasalt – ribbon chert – siltstone succession was overturned (D1) and folded into large-scale, tight to isoclinal antiformal folds (D2). This succession was partly eroded and subsequently covered by cross-bedded sandstones at *c.* 427 Ma or later. This young age contradicts previous correlations of this sedimentary basin with the Ordovician Hovin Groups to the northwest. Post-427 Ma Silurian successions are rare within the record of the Scandinavian Caledonides, but our results together with the findings of Gasser *et al.* (2016) point to a wider extent of such basins than hitherto assumed, opening up for the identification of stratigraphic links between the mostly marine Cambro-Silurian record and the younger Devonian continental Old Red Sandstone facies.

Our study reveals the presence of post-427 Ma intermediate calc-alkaline volcanic/subvolcanic rocks in the Dugurdsknappen area, representing the youngest documented volcanic episode within the TNC so far. Similar rocks are unknown also elsewhere in the Scandinavian Caledonides. The particular geochemical signature of the post-427 Ma volcanic rocks indicates that they are either the result of late-stage subduction zone volcanism just prior to the onset of continent-continent collision, or much younger post-collisional extensional melting influenced by inherited subduction-zone signatures.

All units exposed in the Dugurdsknappen area were affected by a third deformational phase (D3) leading to SW-trending, NW-verging folds and the formation of a regional greenschist facies axial plane foliation. The geometry of this deformation phase indicates a connection to the post-orogenic extensional phase of the Caledonian orogeny after *c.* 400 Ma, rather than to the main Scandian collision and nappe translation.

## Acknowledgments

We thank the Department of Geoscience at the University of Oslo and the Geological Survey of Norway (NGU) for field- and lab work funding. Øyvind Skår and Torkil Røhr Sørlie are thanked for help with U-Pb LA-ICP-MS analyses at the NGU laboratory and discussion of analytical results. David Chew, Rob Strachan and the editor Stephen Daly are thanked for thorough and constructive comments. This work was partly supported by the Research Council of Norway through its Centres of Excellence funding scheme, project number 223272.

## References

Allmendinger, R.W., Cardozo, N.C. & Fisher, D. 2013. *Structural Geology Algorithms: Vectors & Tensors*. Cambridge: Cambridge University Press, 289 pp.

Barnes, C.G., Frost, C.D., Yoshinobu, A.S., McArthur, K., Barnes, M.A., Allen, C.M., ... & Prestvik, T. 2007. Timing of sedimentation, metamorphism and plutonism in the Helgeland Nappe Complex, north-central Norwegian Caledonides. *Geosphere*, 3, 683–703.

Bassett, M. G. 1985. Silurian stratigraphy and facies development in Scandinavia. In: Gee, D.G. & Sturt, B.A. (eds): *The Caledonide Orogen - Scandinavia and Related Areas*. Chichester: John Wiley & Sons, 283-292.

Bingen, B. & Solli, A. 2009. Geochronology of magmatism in the Caledonian and Sveconorwegian belts of Baltica: synopsis for detrital zircon provenance studies. *Norwegian Journal of Geology*, 89(4), 267-290.

Boggs, S.J. 2011. *Principles of Sedimentology and Stratigraphy*. 5th ed. New Jersey: Pearson Education, Inc. 585 pp.

Bruton, D.L. & Bockelie, J.F. 1980. Geology and paleontology of the Hølonda area, western Norway- a fragment of North America? In: Wones, D.R. (eds) *The Caledonides in the USA*. Virginia Polytechnic Geological Sciences Memoir, 2, 41-55.

Bruton, D. L., Gabrielsen, R. H. & Larsen, B. T. 2010. The Caledonides of the Oslo region, Norway – stratigraphy and structural elements. *Norwegian Journal of Geology*, 90, 93–121.

Cardozo, N. & Allmendinger, R.W., 2013, *Spherical projections with OSXStereonet: Computers & Geosciences*, v. 51, no. 0, p. 193 - 205, doi:10.1016/j.cageo.2012.07.021

Chaloupsky, J. 1970. Geology of the Hoelonda-Hulsjoeen area, Trondheim region. *Geological Survey of Norway Bulletin*, 266, 277-304.

Corfu, F., Gerber, M., Andersen, T.B., Torsvik, T.H., & Ashwal, L.D. 2011. Age and significance of Grenvillian and Silurian orogenic events in the Finnmarkian Caledonides, northern Norway. *Canadian Journal of Earth Sciences*, 48, 419-440.

Corfu, F., Andersen, T.B. & Gasser, D. 2014. The Scandinavian Caledonides: main features, conceptual advances and critical questions. In: Corfu, F., Gasser, D. & Chew, D. M. (eds) *New*

*Perspectives on the Caledonides of Scandinavia and Related Areas.* Geological Society, London, Special Publications, 390, 9-43.

Davies, N.S., Turner, P. & Sansom, I.J. 2005. A revised stratigraphy for the Ringerike Group (Upper Silurian, Oslo Region), *Norwegian Journal of Geology*, 85, 193-201.

Davies, N.S., Sansom, I.J. & Turner, P. 2006. Trace Fossils and Paleoenvironments of a Late Silurian Marginal-Marine/Alluvial System: the Ringerike Group (Lower Old Red Sandstone), Oslo Region, Norway. *Palaios*, 21, 46–62.

Dickinson, W.R. & Gehrels, G.E. 2009. Use of U–Pb ages of detrital zircons to infer maximum depositional ages of strata: a test against a Colorado Plateau Mesozoic database. *Earth and Planetary Science Letters*, 288(1), 115-125.

Dilek, Y. & Furnes, H. 2011. Ophiolite genesis and global tectonics: Geochemical and tectonic fingerprinting of ancient oceanic lithosphere. *GSA Bulletin*, 123, 387-411.

Domeier, M. 2016. A plate tectonic scenario for the Iapetus and Rheic oceans. *Gondwana Research*, 36, 275-295.

Dunning, G.R. & Grenne, T. 2000. U-Pb age dating and paleotectonic significance of trondhjemite from the type locality in the Central Norwegian Caledonides. *Geological Survey of Norway Bulletin,* 437, 57-65.

Dunning, G.R. & Pedersen, R.B. 1988. U/Pb ages of ophiolites and arc-related plutons of the Norwegian Caledonides: implications for the development of Iapetus. *Contributions to Mineralogy and Petrology*, 98(1), 13-23.

Fossen, H. 1992. The role of extensional tectonics in the Caledonides of south Norway. *Journal of structural geology*, 14(8), 1033-1046.

Gasser, D., Grenne, T., Corfu, F. & Augland, L.E. 2016. Characterization of depositional age and structure of sedimentary successions by U-Pb TIMS and LA-ICP-MS dating of volcanic horizons and detrital zircons: an example from the western Trondheim Nappe Complex, Scandinavian Caledonides. *Geophysical Research Abstracts*, 18, EGU2016-12961, 2016.

Gee, D.G., Guezou, J.C., Roberts, D. & Wolff, F.C. 1985. The central-southern part of the Scandinavian Caledonides. ln: Gee, D.G. & Sturt, B.A. (eds): *The Caledonide Orogen - Scandinavia and Rel ted Areas.* Chichester: John Wiley & Sons, 109-133.

Gee, D.G., Fossen, H., Henriksen, N. & Higgins, A.K. 2008. From the early Paleozoic platforms of Baltica and Laurentia to the Caledonide Orogen of Scandinavia and Greenland. *Episodes*, 31(1), 44-51.

Gee, D.G., Ladenberger, A., Dahlqvist, P., Majka, J., Be'eri-Shlevin, Y., Frei, D. & Thomsen, T. 2014. The Baltoscandian margin detrital zircon signatures of the central Scandes. *Geological Society, London, Special Publications*, 390(1), 131-155.

Gordon, S.M., Whitney, D.L., Teyssier, C., & Fossen, H. 2013. U-Pb dates and trace-element geochemistry of zircon from migmatite, Western Gneiss Region, Norway: Significance for history of partial melting in continental subduction. *Lithos*, 170-171, 35-53.

Grenne, T. 1989. Magmatic evolution of the Løkken SSZ Ophiolite, Norwegian Caledonides: Relationships between anomalous lavas and high-level intrusions. *Geological Journal*, *24*(4), 251-274.

Grenne, T. & Gasser, D. 2017. The Støren Group greenstones and their relationship to the ophiolite fragments of the western Trondheim Nappe Complex, central Norwegian Caledonides. *Geophysical Research Abstracts*, 19, EGU2017-4901, 2017.

Grenne, T. & Roberts, D. 1998. The Hølonda Porphyrites, Norwegian Caledonides: geochemistry and tectonic setting of Early–Mid-Ordovician shoshonitic volcanism. *Journal of the Geological Society*, *155*(1), 131-142.

Grenne, T., Grammeltvedt, G. & Vokes, F.M. 1980. Cyprus-type sulphide deposits in the western Trondheim district, central Norwegian Caledonides. In: *Ophiolites*. Proceedings of the International Ophiolite Symposium, Cyprus (pp. 727-743).

Grenne, T., Ihlen, P. & Vokes, F. 1999. Scandinavian Caledonide metallogeny in a plate tectonic perspective. *Mineralium Deposita*, 34**,** 422-471.

Harland, W.B. & Gayer, R. A. 1972. The Arctic Caledonides and earlier oceans. *Geological Magazine*, 109(04), 289-314.

Harper, D.A.T., Mac Niocaill, C., & Williams, S.H. 1996. The palaeogeography of early Ordovician Iapetus terranes: an integration of faunal and palaeomagnetic constraints. *Palaeogeography, Palaeoclimatology, Palaeoecology*, 121(3-4), 297-312.

Harris, N. B., Pearce, J. A., & Tindle, A. G. 1986. Geochemical characteristics of collision-zone magmatism. *Geological Society, London, Special Publications*, 19(1), 67-81.

Heim, M., Grenne, T. & Prestvik, T. 1987. The Resfjell ophiolite fragment, Southwest Trondheim Region, Central Norwegian Caledonides. *Geological Survey of Norway Bulletin*, 409, 49-71

Holtedahl, O. 1920. Paleogeography and diastrophism in the Atlantic-Arctic region during Paleozoic time. *American Journal of Science*, (289), 1-25.

Jones, D.L. & Murchey, B. 1986. Geologic significance of Paleozoic and Mesozoic radiolarian chert. *Annual Review of Earth and Planetary Sciences*, 14, 455.

Kylander-Clark, A.R.C., & Hacker, B.R. 2014. Age and significance of felsic dikes from the UHP western gneiss region. *Tectonics*, 33, 2342-2360.

Lancaster, P. J., Strachan, R. A., Bullen, D., Fowler, M., Jaramillo, M., & Saldarriaga, A. M. 2017. U–Pb zircon geochronology and geodynamic significance of 'Newer Granite'plutons in Shetland, northernmost Scottish Caledonides. *Journal of the Geological Society*, 174(3), 486-497.

Le Bas, M.J., Le Maitre, R.W., Streckeisen, A. & Zanettin, B. 1986. A chemical classification of volcanic rocks based on the total alkali-silica diagram. *Journal of petrology*, 27(3), 745-750.

Mac Niocaill, C., Van der Pluijm, B.A. & Van der Voo, R. 1997. Ordovician paleogeography and the evolution of the Iapetus ocean. *Geology*, 25, 159-162.

Miles, A.J., Woodcock, N.H. & Hawkesworth, C.J. 2016. Tectonic controls on post-subduction granite genesis and emplacement: The late Caledonian suite of Britain and Ireland. *Gondwana Research*, 39, 250–260

Nesse, W.D. 2013. *Introduction to Optical Mineralogy*.4th ed. Oxford: Oxford University Press. 361 pp.

Neuman, R.B. 1984. Geology and paleobiology of islands in the Ordovician Iapetus Ocean: review and implications. *GSA Bulletin*, 95, 1188-1201.

Neuman, R.B. & Bruton, D.L. 1989. Brachiopods and trilobites from the Ordovician Lower Hovin Group (Arenig/Llanvirn), Hølonda area, Trondheim region, Norway: new and revised taxa and paleogeographic interpretation. *Geological Survey of Norway Bulletin*, 414, 49-89.

Neuman, R.B., Bruton, D.L. & Pojeta, J. 1997. Fossils from the Ordovician "Upper Hovin Group" (Caradoc–Ashgill), Trondheim region, Norway. *Geological Survey of Norway Bulletin*, 432, 25–58.

Nilsen, O. & Wolff, F.C. 1989. *Geological map of Norway, bedrock map Røros & Sveg, 1:250 000*, Trondheim: Geological Survey of Norway

Nilsen, O., Corfu, F. & Roberts, D. 2007. Silurian gabbro-diorite-trondhjemite plutons in the Trondheim Nappe Complex, Caledonides, Norway: petrology and U-Pb geochronology. *Norwegian Geological Journal*, 87(3), 329.

Oftedahl, C. 1980. Excursion guide Day 8, Støren-Horg-Hølonda. *Geological Survey of Norway Bulletin*, 356, 151-159

Oftedahl, C. & Prestvik, T. 1985. *Continental margin pyroclastics and the stratigraphy of the 'Horg Syncline'*. University of Trondheim, the Norwegian Institute of Technology.

Pearce, J.A. 1982. Trace element characteristics of lavas from destructive plate boundaries. *Andesites*, 8, 525-548.

Pearce, J.A. 1983. The role of sub-continental lithosphere in magma genesis at destructive plate margins. In: C. J. Hawkesworth & M. J. Norry (eds). *Continental basalts and mantle xenoliths.*, 230-49. Nantwich: Shiva

Pearce, J.A. & Cann, J.R. 1973. Tectonic setting of basic volcanic rocks determined using trace element analyses. *Earth and planetary science letters*, 19(2), 290-300.

Pedersen, R.B., Bruton, D.L. & Furnes, H. 1992. Ordovician faunas, island arcs and ophiolites in the Scandinavian Caledonides. *Terra Nova*, 4(2), 217-222.

Pufahl, P.K. 2010. Bioelemental Sediments. In: James, N.P. & Dalrymple, R.W. (eds) *Facies Models 4*,GEOtext 6 Geological Association of Canada, Newfoundland and Labrador, Canada, p. 477-503

Roberts, D. 2003. The Scandinavian Caledonides: event chronology, palaeogeographic settings and likely modern analogues. *Tectonophysics*, 365(1), 283-299.

Roberts, D. & Stephens, M. 2000. Caledonian orogenic belt. Description to the bedrock map of central Fennoscandia (Mid-Norden). *Geological Survey of Finland Special Paper,* 28**,** 78-104.

Roberts, D. & Wolff, F. 1981. Tectonostratigraphic development of the Trondheim region Caledonides, central Norway. *Journal of Structural Geology,* 3**,** 487-494.

Roberts, D., Grenne, T. & Ryan, P.D. 1984. Ordovician marginal basin development in the central Norwegian Caledonides. *Geological Society, London, Special Publications,* 16, 233-244.

Roberts, D., Walker, N., Slagstad, T., Solli, A. & Krill, A. 2002. U-Pb zircon ages from the Bymarka ophiolite, near Trondheim, central Norwegian Caledonides, and regional implications. *Norwegian Geological Journal*, *82*(1), 19-30.

Rohr-Torp, E. 1972. A major inversion of the western part of the Trondheim Nappe. *Norwegian Geological Journal*, 52, 453-458.

Rohr-Torp, E. 1974. Contact metamorphism around the Innset massif. *Norwegian Geological Journal*, 54, 13-33.

Slagstad, T. 2003. Geochemistry of trondhjemites and mafic rocks in the Bymarka ophiolite fragment, Trondheim, Norway: petrogenesis and tectonic implications. *Norwegian Geological Journal*, *83*(3), 167-185.

Slagstad, T., Pin, C., Roberts, D., Kirkland, C., Grenne, T., Dunning, G., Sauer, S. & Andersen, T. 2013. Tectonomagmatic evolution of the Early Ordovician suprasubduction-zone ophiolites of the Trondheim Region, Mid-Norwegian Caledonides. *Geological Society, London, Special Publications*, 390(1), pp.541-561.

Solli, A. & Nordgulen, Ø. 2013. *Bedrock map of Norway and the Caledonides of Sweden and Finland, 1:2 000 000,* Trondheim: Geological Survey of Norway

Song, S., Wang, M., Wang, C., & Niu, Y. 2015. Magmatism during continental collision, subduction, exhumation and mountain collapse in collisional orogenic belts and continental net growth: A perspective. *Science China Earth Sciences*, 58(8), 1284-1304.

Soper, N.T. & Woodcock, N.H. 1990. Silurian collision and sediment dispersal patterns in southern Britain. *Geological Magazine*, 127(06), 527-542.

Sun, S. & McDonough, W. 1989. Chemical and isotopic systematics of oceanic basalts: implications for mantle composition and processes. *Geological Society, London, Special Publications*, 42(1), pp.313-345.

Torsvik, T.H. & Trench, A. 1991. The Ordovician history of the Iapetus Ocean in Britain: new paleomagnetic constraints. *Journal of the Geological Society, London*, 148, 423-425.

Tucker, M.R. 2001. *Sedimentary Petrology.* 3rd ed. United Kingdom: Blackwell Science. 262 pp.

Vogt, T. 1945. The geology of part of the Hølonda-Horg district, a type area in the Trondheim region. *Norwegian Geological Journal*, *25*, 449-528.

Walsh, J.J. 1986. The geology and structure of the Horg Syncline, southeast of Meldal, Sør-Trøndelag, Norway, *Geological Survey of Norway Bulletin*, 406, 57–66.

Wilson, J.T. 1966. Did the Atlantic close and then re-open? *Nature*, 211, 676-681.

Wilson, M. 1989. *Igneous Petrology: A global tectonic approach*. 1st ed. London:Chapman & Hall. 466 pp.

Winter, J.D. 2010. *Principles of Igneous and Metamorphic Petrology.* 2nd ed. New Jersey: Pearson Education. 702 pp.

Wolff, F.C. 1976. *Geological map of Norway, bedrock map Trondheim, 1:250 000.* Trondheim: Geological Survey of Norway.

Wolff, F.C. 1979. Beskrivelse til de berggrunnsgeologiske kart Trondheim og Østersund 1:250 000 (med fargetrykt kart).,NGU; Skrifter 353, 1-76 + kar

Wood, D.A. 1980. The application of a Th Hf Ta diagram to problems of tectonomagmatic classification and to establishing the nature of crustal contamination of basaltic lavas of the British Tertiary Volcanic Province. *Earth and planetary science letters*, *50*(1), 11-30.

**Figures**

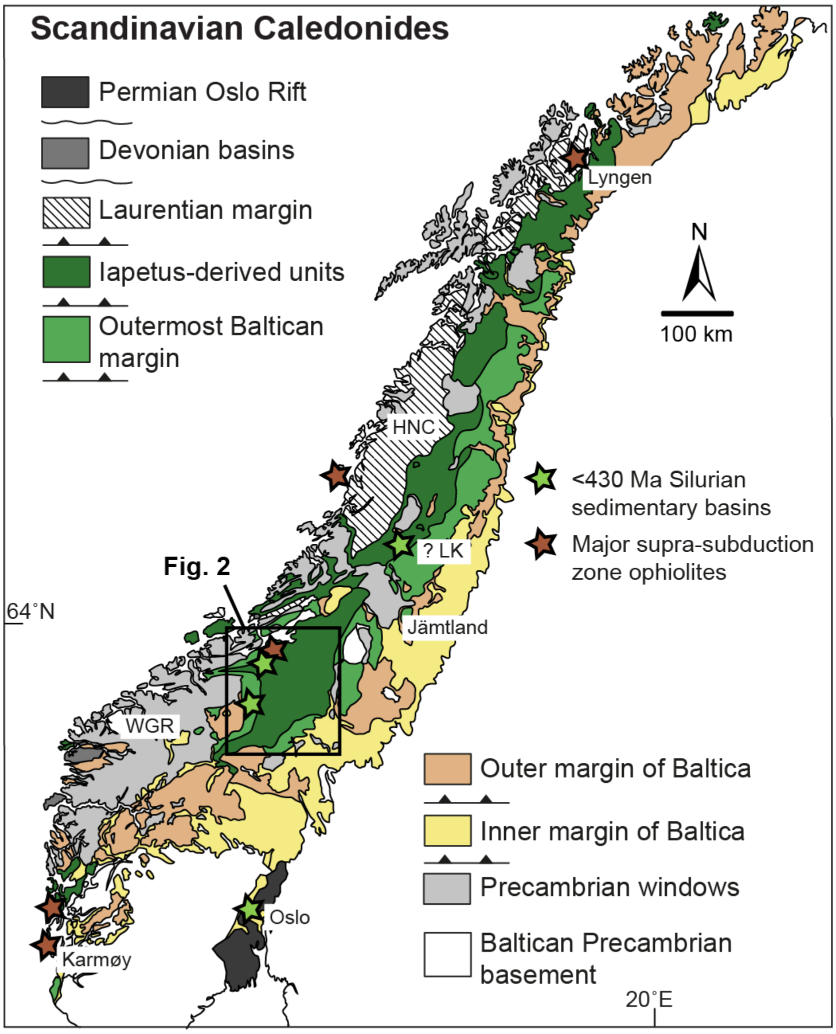


**Fig. 1:** Simplified tectonostratigraphic map of western Scandinavia showing the main paleogeographic domains within the Caledonian nappe stack of Scandinavia, simplified after Solli & Nordgulen (2013). Remnants of the Iapetus Ocean are shown in dark green. Rectangle shows approximate extent and position of the Trondheim Nappe Complex (Fig. 2). The distribution of larger supra-subduction zone (SSZ) ophiolites and the occurrences of <430 Ma Silurian sedimentary basins are indicated. WGR, Western Gneiss Region; HNC, Helgeland Nappe Complex; LK, Lower Köli Nappes.

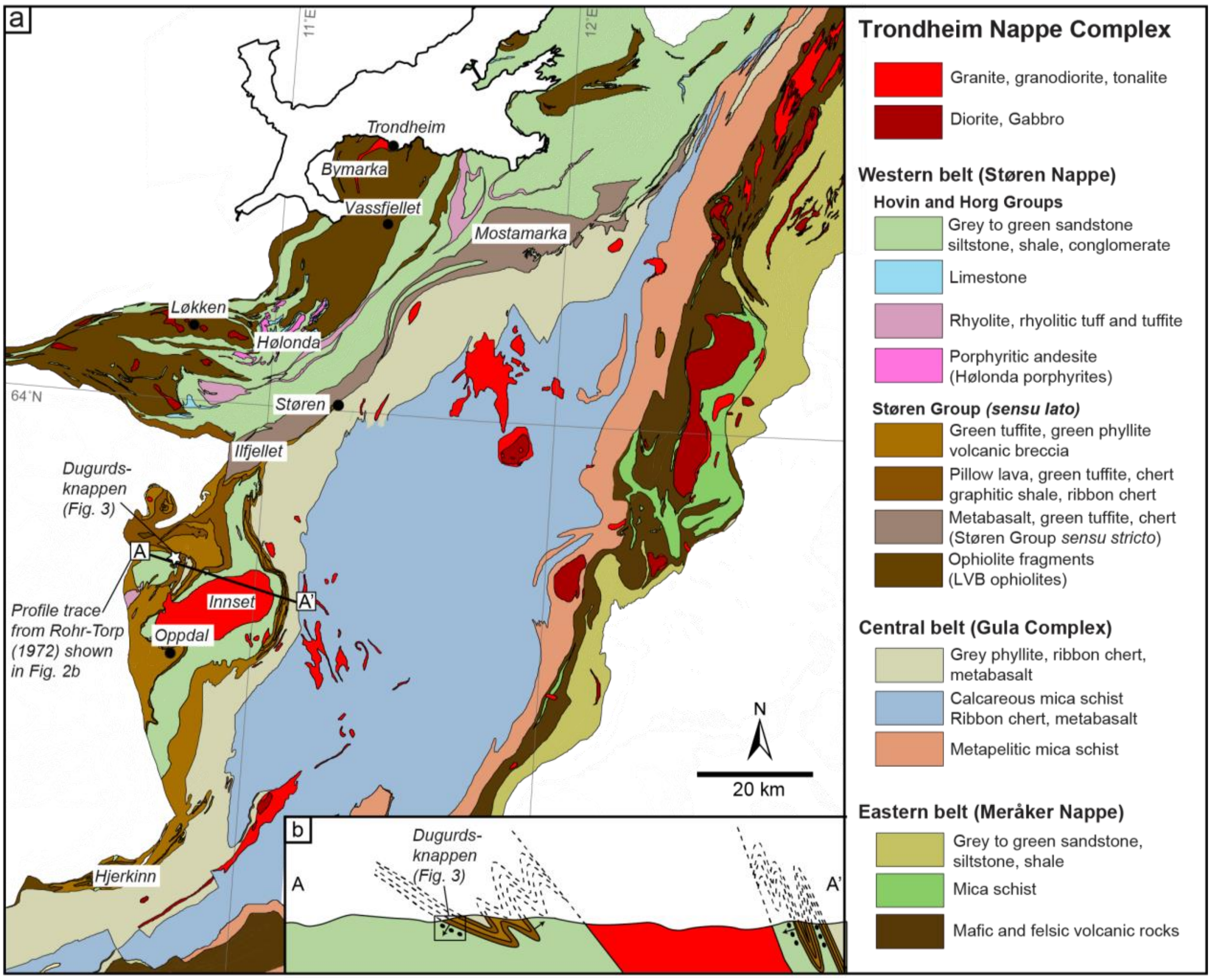


**Fig. 2:** (**a**) Geological map of the Trondheim Nappe Complex showing the western, central and eastern belts, map modified from Nilsen & Wolff (1989) and Wolff (1976). Location of the study area (Fig. 3) is indicated by a small star at Dugurdsknappen in the southern part of the western belt, where also the extent of the profile A-A' (Fig. 2b) is shown. (**b**) Profile A-A' from Rohr-Torp (1972) indicates overturning and isoclinal folding of the volcanic and sedimentary succession in the southern part of the western TNC.

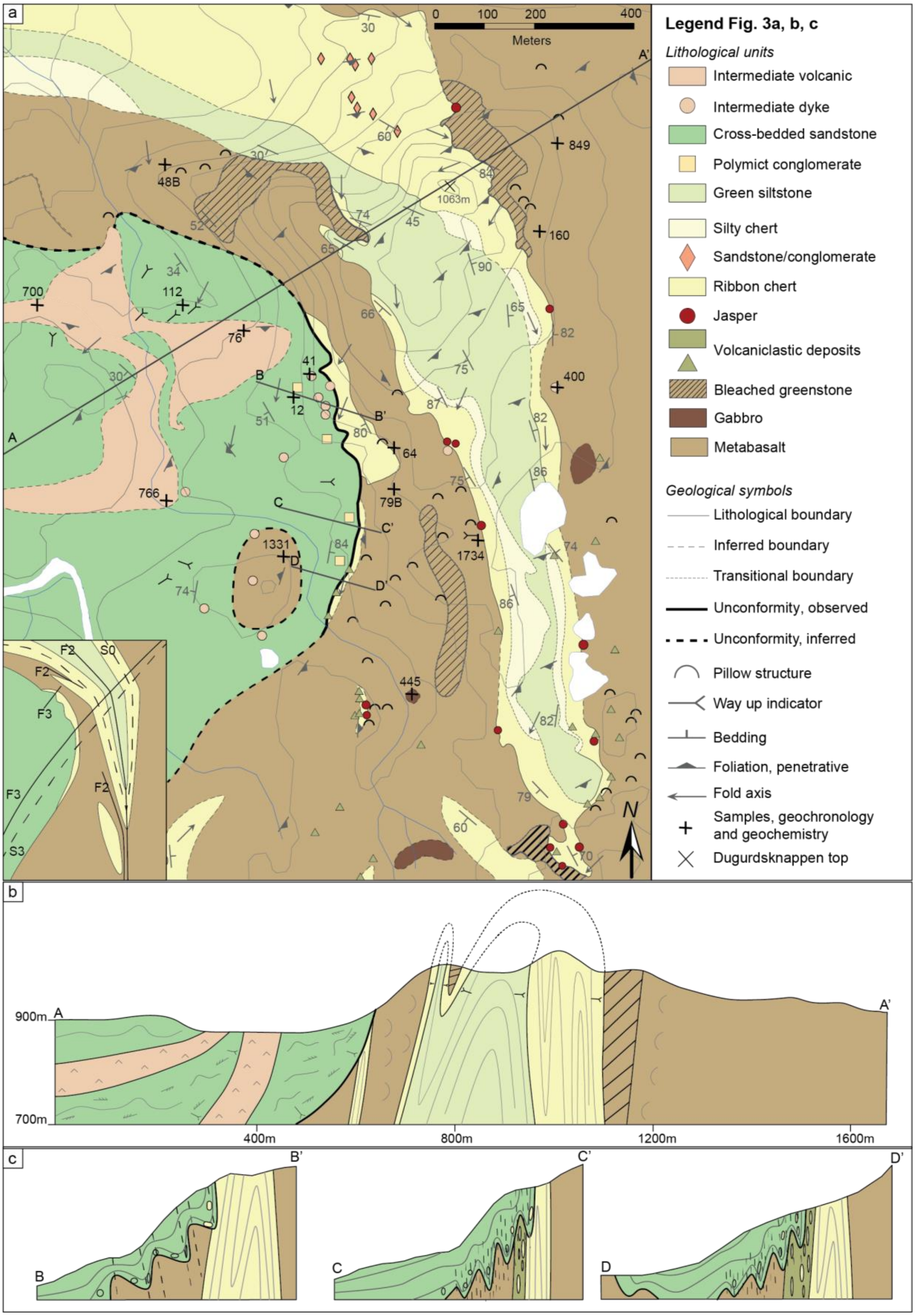


Fig. 3: **(a)** Geological map of the Dugurdsknappen area. Small inset map (lower left) shows our structural interpretation of the study area. **(b)** Cross section A-A' shows the large-scale

structure of the area, while **(c)** cross sections B-B’, C-C’ and D-D’ show variably deformed parts of the unconformity.

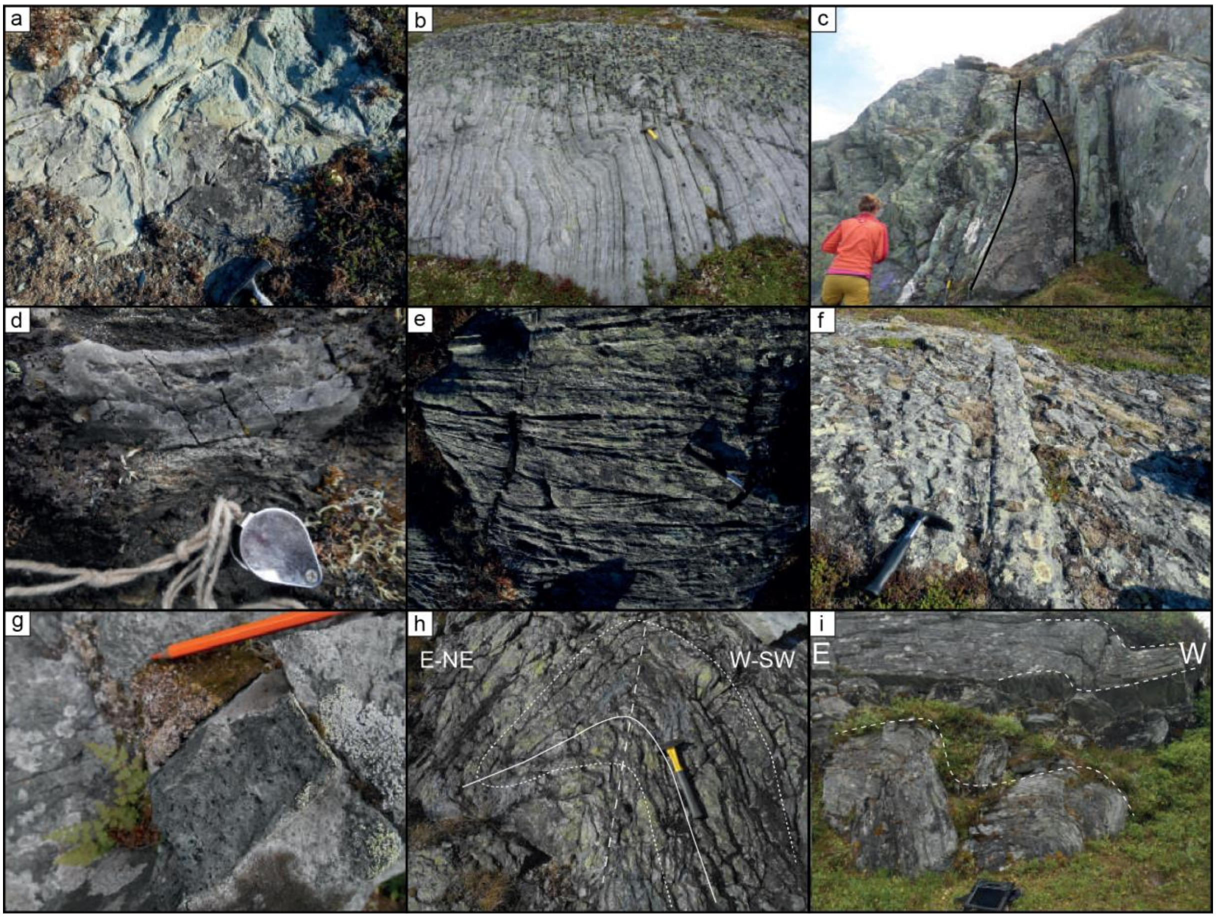


**Fig. 4:** Field photographs from the Dugurdsknappen area. (**a**) Pillow lava. (**b**) Folded ribbon chert. (**c**) Bed of immature sandstone (between black lines) within the ribbon chert. (**d**) Angular chert clast within the basal part of the cross-bedded sandstone. (**e**) Cross bedded sandstone. (**f**) Intermediate dyke cutting the metabasalt below the unconformity. (**g**) Close-up of the intermediate volcanic rock. Note the porphyritic texture with biotite phenocrysts. **(h)** Refolded fold within the ribbon chert, indicating the presence of two distinct fold phases with the younger phase representing W-verging folds. (**i**) W-NW-verging folds within the cross-bedded sandstone.

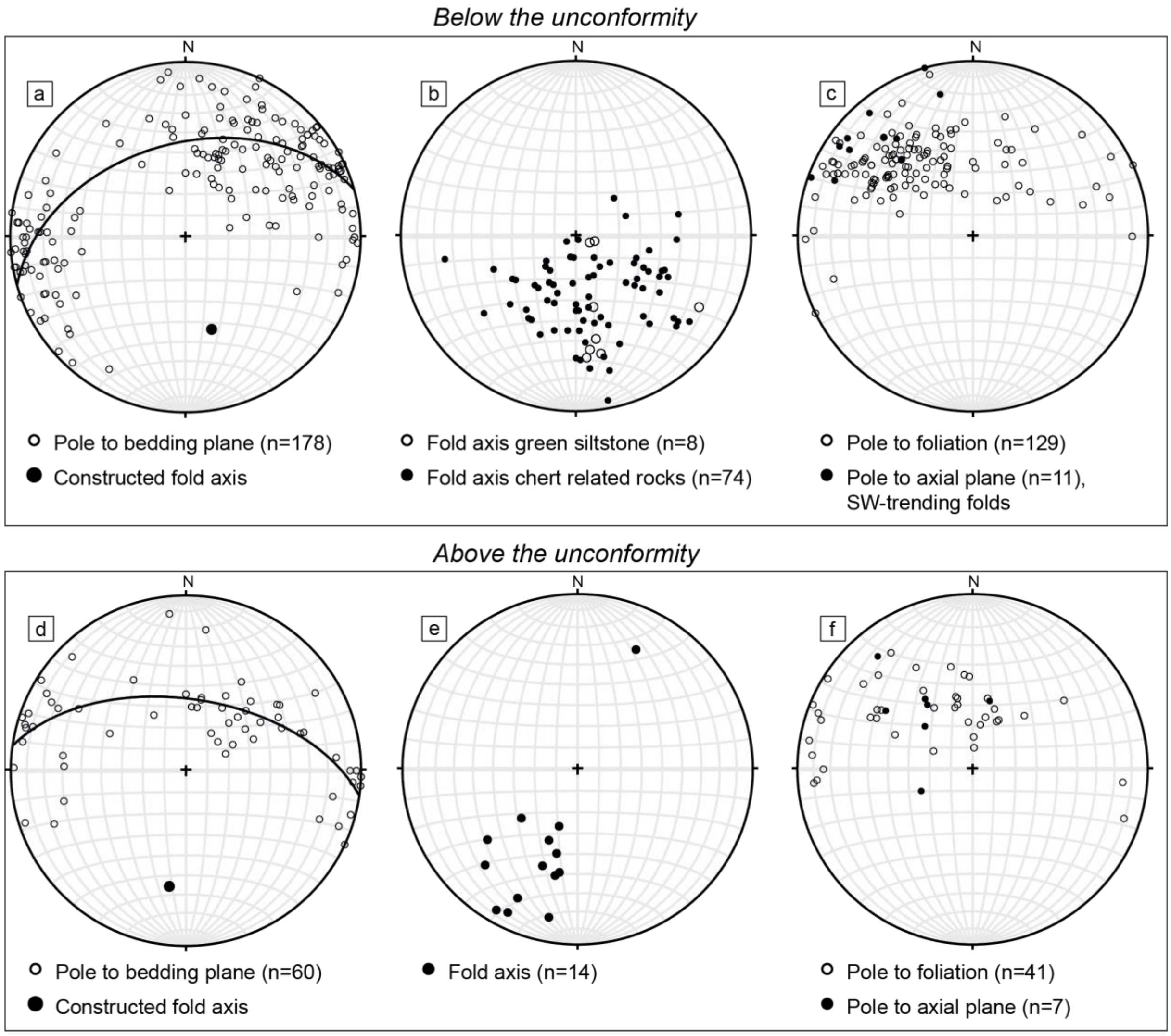


**Fig. 5:** Structural data from the Dugurdsknappen area presented in equal-area lower hemisphere stereoplots (produced with Stereonet 8; Cardozo & Allmendinger 2013; Allmendinger *et al.* 2013). (**a**) Poles of bedding planes in units below the unconformity (mainly from chert- and siltstone-related rocks) and the constructed large-scale fold axis plunging moderately to the SE. (**b**) Fold axis measurements from outcrop-scale folds below the unconformity. (**c**) Poles to foliation and to axial planes of SW-trending folds measured below the unconformity. (**d**) Poles to bedding planes above the unconformity, indicating the constructed large-scale fold axis plunging moderately to the S-SW. (**e**) Fold axes measured above the unconformity. (**f**) Poles to foliation and to axial planes of all folds above the unconformity

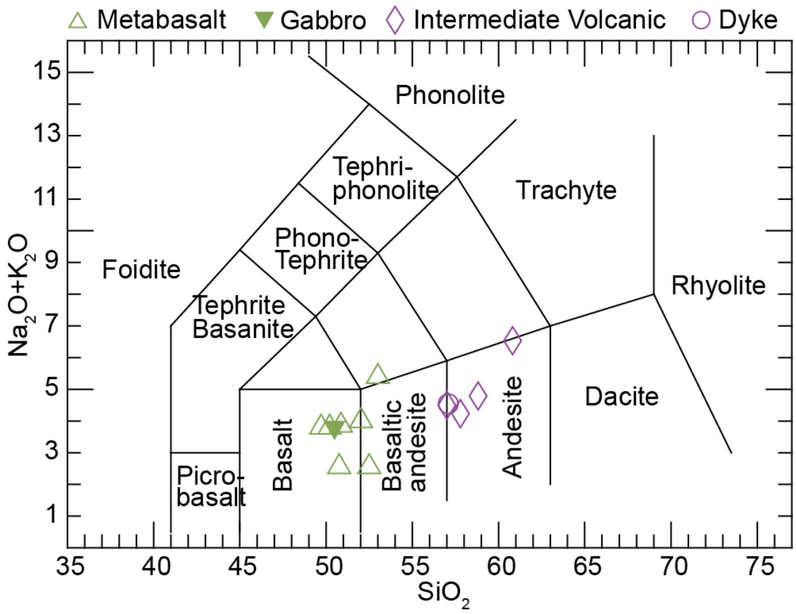


**Fig. 6:** TAS-diagram (Le Bas *et al.* 1986) showing the total alkalis versus silica of the igneous rocks below and above the unconformity at Dugurdsknappen. Values from Table 1 normalized to 100% on a volatile-free basis.

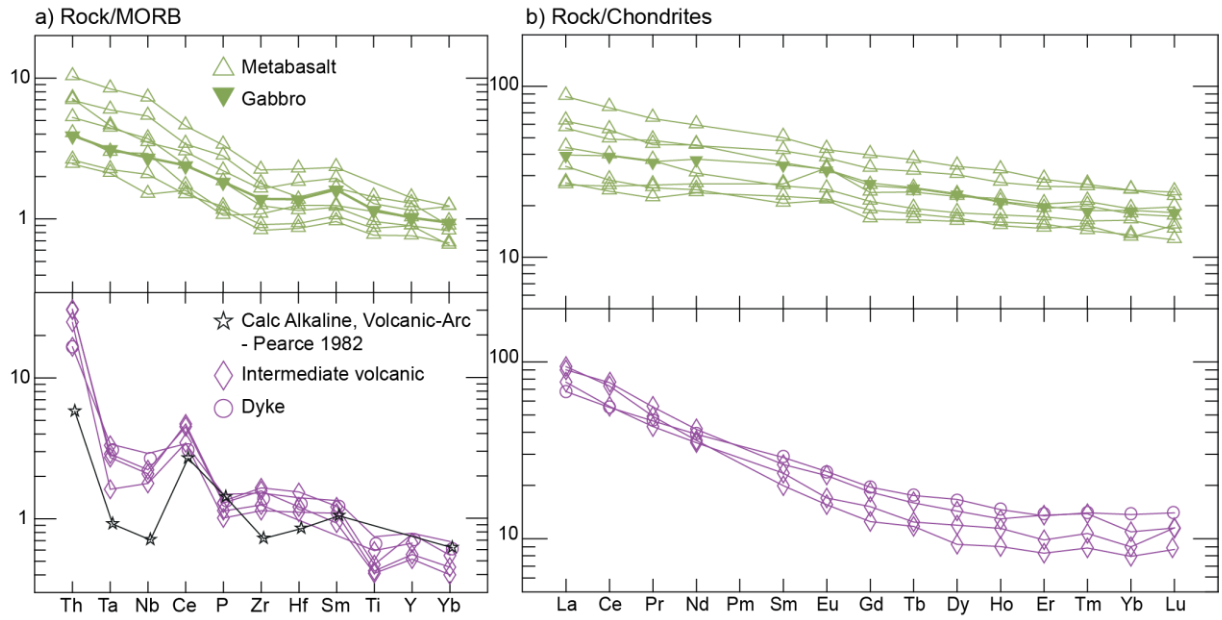


**Fig. 7:** Multi-element plots for immobile incompatible trace elements and REE from the igneous rocks at Dugurdsknappen. (**a**) MORB-normalized trace element diagrams, including a typical calc-alkaline volcanic arc basalt (Pearce 1982) for comparison. Normalization values from Pearce (1983). (**b**) Chondrite-normalized REE plots; chondrite values from Sun and McDonough (1989).

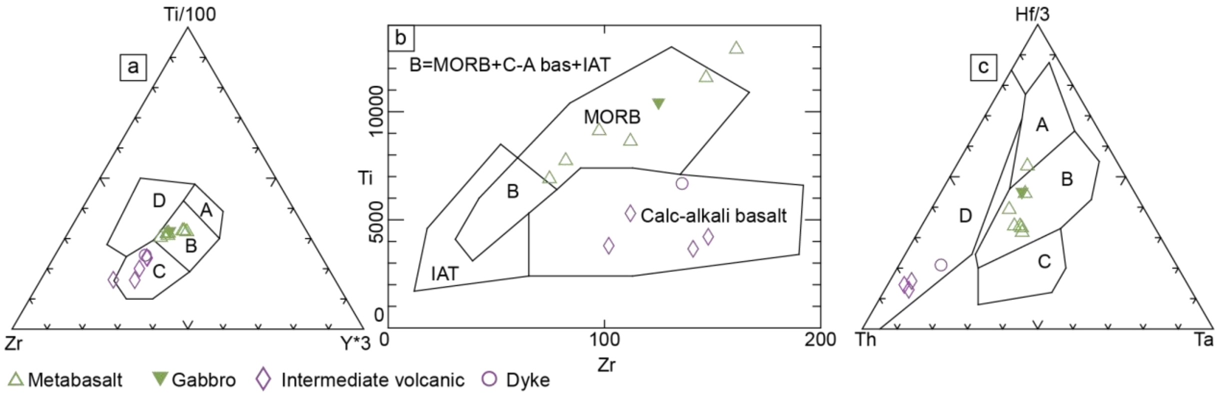


**Fig. 8:** Discrimination diagrams based on trace element concentrations from the igneous rocks at Dugurdsknappen. (**a**) Zr-Y-Ti discrimination diagram (Pearce and Cann 1973). A+B, island arc tholeiites; B, ocean-floor tholeiites; B+C, calc-alkali basalts; D, within-plate basalts. (**b**) Ti vs. Zr discrimination diagram (Pearce and Cann 1973). MORB, mid-ocean ridge basalts; IAT, island arc tholeiites; B, MORB+IAT+calc-alkali basalts. Note: diagram a and b are intended for basaltic rocks, the intermediate rocks are plotted for comparison. (**c**) Th-Ta-Hf discrimination diagram (Wood 1980). A, normal mid-ocean basalts (N-MORB); B, enriched mid-ocean ridge basalts (E-MORB); C, ocean island basalts (OIB); D, volcanic arc basalts.

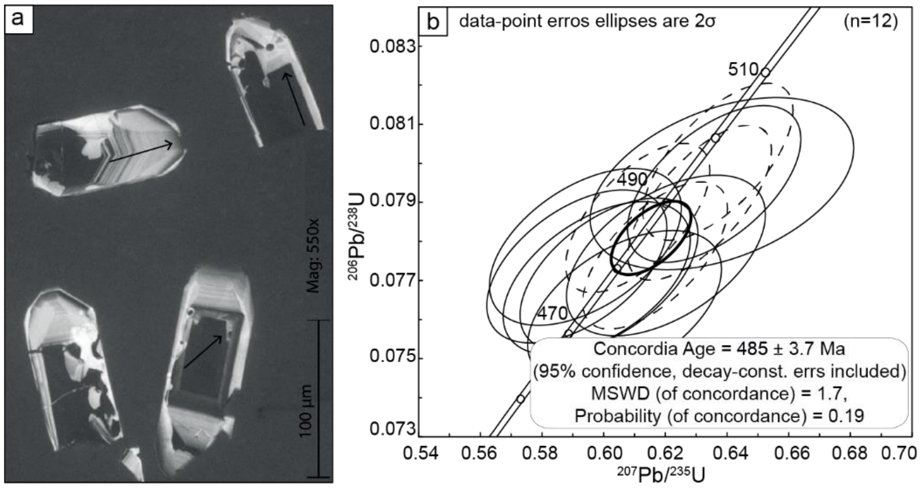


**Fig. 9:** (**a**) CL images of representative zircons from the tonalitic clast sample EST_12. Arrows indicate position and orientation of LA-ICP-MS line analysis (15µm line width). (**b**) Concordia plot for sample EST_12.  Dashed lines are from the cores and solid from the rims, yielding an age of intrusion at 485 ± 4 Ma.

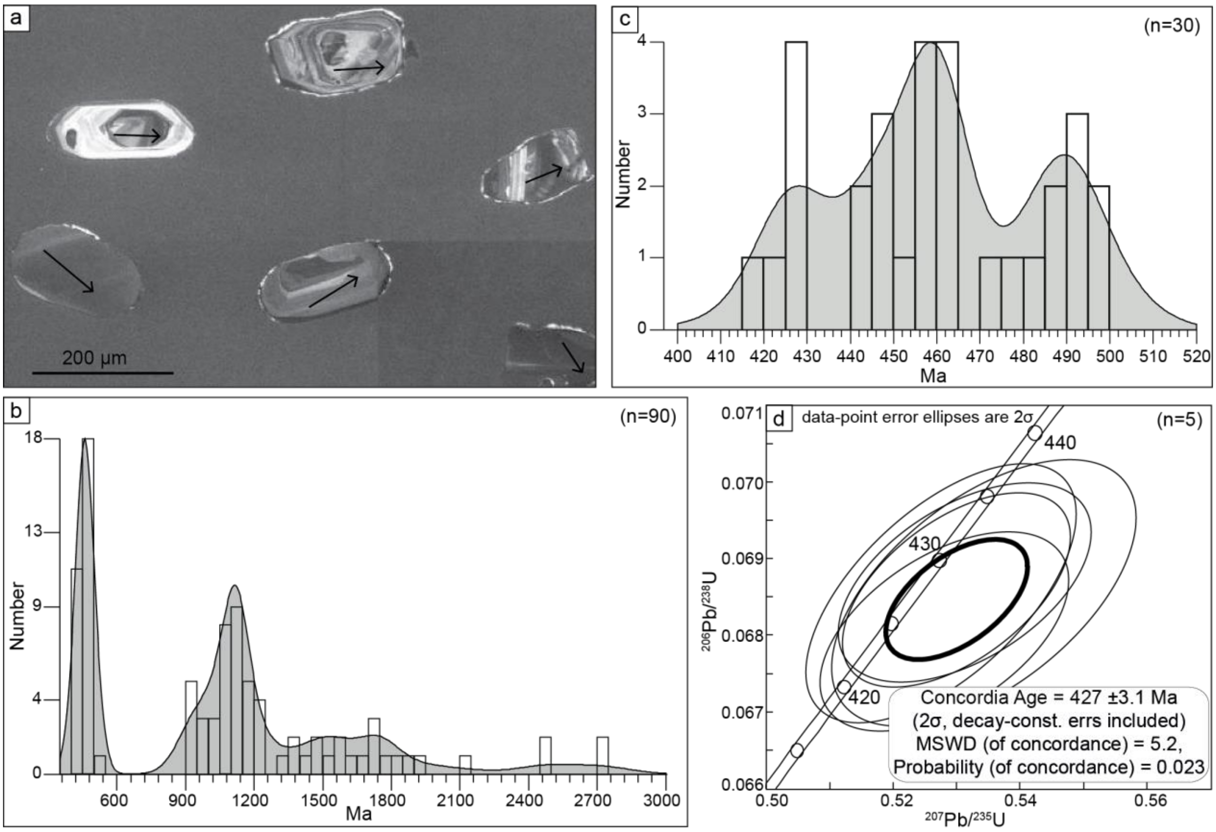


**Fig. 10:** (**a**) CL images of representative zircons from the cross-bedded sandstone sample EST_112. Arrows indicate position and orientation of LA-ICP-MS line analysis (15µm line width). (**b**) Kernel density estimate and histogram of all analyses from ~400-3000 Ma. (**c**) Kernel density estimate and histogram of the Caledonian age group, with minor peaks at about 430, 460 and 490 Ma. (**d**) Concordia plot of the youngest overlapping population of five grains yielding a Concordia age of 427 ± 3 Ma, which indicates the maximum depositional age for the cross-bedded sandstone.

**Table 1:** *Major (wt %) and trace (ppm) elements from whole-rock analyses on XRF[1] and ICP-MS[2]. Sample location indicated in Fig. 3a.*

| | Metabasalt and gabbro* below the unconformity | | | | | | | | Dyke† | Intermediate volcanic/subvolcanic rocks above the unconformity | | | |
|---|---|---|---|---|---|---|---|---|---|---|---|---|---|
| **Sample** | **EST_48B** | **EST_64** | **EST_79B** | **EST_160** | **EST_849** | **15BD 1331** | **15BD 1734** | **EST_445*** | **EST_400** | **EST_41** | **EST_766** | **EST_700** | **EST_76** |
| $SiO_2$[1] (wt%) | 50.4 | 47.9 | 47.6 | 48.4 | 48.5 | 48.50 | 49.80 | 48.6 | 52.5 | 56.1 | 55.2 | 55.2 | 57.8 |
| $TiO_2$[1] | 1.15 | 1.44 | 1.93 | 2.15 | 1.29 | 1.47 | 2.29 | 1.74 | 1.11 | 0.703 | 0.884 | 0.634 | 0.61 |
| $Al_2O_3$[1] | 15.9 | 15.5 | 15.2 | 16.3 | 14.4 | 13.00 | 15.10 | 14.3 | 14.2 | 16.2 | 16.5 | 14.3 | 15.6 |
| $Fe_2O_3$[1] | 8.07 | 9.28 | 10.3 | 10.7 | 8.55 | 8.t99 | 10.80 | 9.51 | 5.27 | 7.11 | 7.9 | 7.54 | 5.38 |
| FeO[1] | 7.3 | 8.4 | 9.3 | 9.6 | 7.7 | | | 8.6 | 4.7 | 6.4 | 7.1 | 6.8 | 4.8 |
| MnO[1] | 0.121 | 0.157 | 0.163 | 0.148 | 0.174 | 0.14 | 0.18 | 0.195 | 0.151 | 0.118 | 0.134 | 0.141 | 0.092 |
| MgO[1] | 6.41 | 8.62 | 7.95 | 6.99 | 7.72 | 9.17 | 6.77 | 10 | 2.61 | 6.56 | 5.06 | 7.02 | 4.95 |
| CaO[1] | 10.8 | 8.67 | 8.69 | 7.89 | 10.9 | 12.70 | 5.75 | 8.03 | 11.8 | 3.81 | 6.49 | 6.52 | 4.24 |
| $Na_2O$[1] | 3.67 | 3.3 | 3.35 | 2.39 | 3.58 | 2.13 | 4.58 | 3.33 | 3.8 | 3.21 | 2.89 | 2.84 | 4.01 |
| $K_2O$[1] | 0.201 | 0.316 | 0.309 | 0.04 | 0.091 | 0.20 | 0.70 | 0.328 | 0.325 | 1.41 | 1.5 | 1.2 | 2.2 |
| $P_2O_5$[1] | 0.141 | 0.225 | 0.269 | 0.343 | 0.15 | 0.13 | 0.40 | 0.225 | 0.181 | 0.162 | 0.138 | 0.123 | 0.157 |
| LOI[1] | 2.66 | 3.16 | 3.06 | 3.89 | 3.92 | 2.59 | 2.65 | 3.15 | 6.97 | 4.01 | 2.56 | 2.54 | 3.62 |
| Th[2] (ppm) | 0.807 | 1.05 | 1.43 | 1.39 | 0.524 | 0.477 | 1.98 | 0.783 | 3.3 | 6.09 | n.a. | 4.92 | 6.01 |
| Ta[2] | 0.537 | 0.796 | 0.827 | 1.07 | 0.404 | 0.371 | 1.46 | 0.563 | 0.606 | 0.486 | n.a. | 0.289 | 0.515 |
| Nb[2] | 10.2 | 13 | 12.2 | 18.8 | 7.24 | 5.05 | 24.4 | 9.53 | 10.1 | 7.24 | n.a. | 6.19 | 7.74 |
| Zr[1] | 74.6 | 112 | 147 | 161 | 82.1 | 94.1 | 193.0 | 125 | 136 | 148 | 112 | 102 | 141 |
| Hf[2] | 2.06 | 2.75 | 4.37 | 3.43 | 2.23 | 2.89 | 5.24 | 3.31 | 3.36 | 3.69 | n.a. | 2.65 | 2.89 |
| Y[1] | 22.8 | 26.8 | 34.5 | 38.7 | 26.9 | 29.50 | 40.9 | 30.6 | 23.5 | 23.2 | 20 | 16.6 | 15.4 |
| La[2] | 8.06 | 10.4 | 13.5 | 14.8 | 6.45 | 6.06 | 19.9 | 9.4 | 16.1 | 21.4 | n.a. | 18.2 | 22.3 |
| Ce[2] | 17.3 | 24.2 | 30 | 34 | 14.9 | 15.7 | 44.2 | 24 | 33.8 | 46.7 | n.a. | 34.3 | 44.7 |
| Pr[2] | 2.42 | 3.49 | 4.59 | 4.33 | 2.11 | 2.42 | 5.93 | 3.44 | 4.4 | 5.28 | n.a. | 4.09 | 4.67 |
| Nd[2] | 11.6 | 14.5 | 21 | 21.2 | 11.1 | 12.10 | 26.70 | 17.5 | 18.2 | 19.4 | n.a. | 16.3 | 16.8 |
| Sm[2] | 3.16 | 4 | 6.42 | 5.47 | 3.47 | 3.96 | 7.38 | 5.33 | 4.41 | 4.02 | n.a. | 3.59 | 3.05 |
| Eu[2] | 1.25 | 1.45 | 2.21 | 1.88 | 1.27 | 1.86 | 2.38 | 1.89 | 1.39 | 1.32 | n.a. | 0.986 | 0.903 |
| Gd[2] | 3.43 | 4.36 | 6.78 | 5.39 | 3.88 | 4.74 | 7.85 | 5.59 | 4.02 | 3.77 | n.a. | 3.12 | 2.57 |
| Tb[2] | 0.619 | 0.721 | 1.19 | 0.943 | 0.671 | 0.87 | 1.34 | 0.956 | 0.657 | 0.597 | n.a. | 0.465 | 0.439 |
| Dy[2] | 4.11 | 4.62 | 7.73 | 5.89 | 4.31 | 5.54 | 8.33 | 5.99 | 4.24 | 3.64 | n.a. | 3.03 | 2.36 |
| Ho[2] | 0.908 | 1 | 1.55 | 1.19 | 0.864 | 1.21 | 1.76 | 1.2 | 0.826 | 0.733 | n.a. | 0.647 | 0.511 |
| Er[2] | 2.59 | 2.85 | 4.3 | 3.19 | 2.44 | 3.27 | 4.55 | 3.29 | 2.23 | 2.25 | n.a. | 1.63 | 1.37 |
| Tm[2] | 0.364 | 0.415 | 0.657 | 0.51 | 0.39 | 0.52 | 0.657 | 0.477 | 0.357 | 0.353 | n.a. | 0.273 | 0.226 |
| Yb[2] | 2.3 | 2.8 | 4.18 | 3.04 | 2.22 | 3.14 | 4.05 | 3.2 | 2.33 | 1.86 | n.a. | 1.53 | 1.35 |
| Lu[2] | 0.321 | 0.369 | 0.574 | 0.44 | 0.391 | 0.48 | 0.59 | 0.463 | 0.356 | 0.292 | n.a. | 0.293 | 0.221 |

† Intermediate dyke from below the unconformity. n.a., not analysed